Experimental Demonstration of Bistatic UAV-Borne SAR and InSAR

Se-Yeon Jeon[a], Brian Hawkins[a], Samuel Prager[a], Matthew Anderson[b], Stefano Moro[c], Eric Loria[a], Robert Beauchamp[a], Soon-Jo Chung[a,b], Marco Lavalle[a]
[a]Jet Propulsion Laboratory, California Institute of Technology, Pasadena, CA, USA
[b]California Institute of Technology, Pasadena, CA, USA
[c]Politecnico di Milano, Milan, Italy

Abstract

The Distributed Aperture Radar Tomographic Sensors (DARTS) project at the NASA Jet Propulsion Laboratory aims to mature and demonstrate multi-static SAR measurements for fine-scale 3D imaging of surface topography, vegetation, and surface deformation and change. This project explores the use of drones as SAR platforms and integrates software-defined radar on RF system-on-chip for compact and flexible radar instruments. This paper highlights the progress in DARTS hardware development, experiments, and data processing. Recent experiments have successfully demonstrated monostatic interferometry as well as acquisition and processing of bi-static SAR imagery. By leveraging the advantages of multi-static SAR and drone-based and airborne platforms, the project aims to build a testbed for future mission design and enhanced SAR imaging capabilities for scientific applications.

1 Introduction

Synthetic aperture radar (SAR) has emerged as a prominent imaging technology extensively utilized in all-weather remote sensing applications, offering significant benefits to a broad range of scientific disciplines [1]. Traditionally operating in a two-dimensional domain, SAR has undergone advancements that extend its capabilities in the cross-track/elevation direction, enabling three-dimensional (3D) volumetric imaging. This technique, known as SAR tomography or TomoSAR [2], has garnered increased attention for its potential in the engineering and scientific remote sensing field.

The application of interferometric SAR (InSAR) and tomographic SAR in a bi- and multi-static operational setting, utilizing spatially separated transmit and receive elements, presents an effective solution to the challenges posed by temporal decorrelation. These techniques offer enhanced robustness to temporal variations that typically hinder repeat-pass interferometric measurements particularly over vegetated landscapes [3, 4].

In recent years, the utilization of small uninhabited aerial vehicles (UAV) as SAR platforms has gained substantial attention due to their unique capabilities and versatility. UAVs offer the potential for immediate access to target area and flexible trajectory planning, making them ideal for SAR experiments that requires frequent measurements.

The Distributed Aperture Radar Tomographic Sensors (DARTS) is a project led by the NASA Jet Propulsion Laboratory in collaboration with the California Institute of Technology (Caltech). The primary objective of the DARTS project is to advance fine-scale imaging of 3D surface topography and vegetation (STV) analysis with benefits also for surface deformation and change (SDC) monitoring [5]. To achieve this, the DARTS team has been conducting experiments to showcase the capabilities of drone-based SAR imaging [6]. The integration of software-defined radar (SDRadar) implemented on RF system-on-chip (RFSoC) [7] has enabled the reduction in size, mass, power, and cost of future airborne and spaceborne radar instruments. In this paper, we present the latest progress made in the development of the DARTS UAV hardware, as well as the conducted experiments and data processing employed in the project.

2 UAV-SDRadar Testbed

An ultra-wideband SDRadar testbed has been developed using a battery-powered embedded system based on the Xilinx RFSoC, enabling compact and flexible radar architectures. The SDRadar is capable of multiband operations and is implemented using the Alpha Data ADM-XRC-9R1 based on the Xilinx Zynq UltraScale+ RFSoC with a field programmable gate array (FPGA) and a quad-core ARM processing system for both hardware and software programmability. The RFSoC features 8x 6.4 GSPS digital-to-analog converters and 8x 4 GSPS analog-to-digital converters. The SDRadar is configured to operate at L-band and S-band for the DARTS experiments. The hardware of the RFSoc-based SDRadar testbed is shown in Figure 1.

An Aurelia X6 hexacopter is used to fly the 4.5 kg payload at up to ~100 m above ground level. To transmit and receive the radar signals, two RFSpace TSA600 Vivaldi antennas with an operating frequency of 600-6000 MHz are mounted using a carbon fiber boom with adjustable off-nadir angle of $45° \pm 10°$. Radar-absorbent foam was inserted between the transmit and receive antennas to help minimize direct path signals. The integrated DARTS testbed in operation is shown in Figure 2.

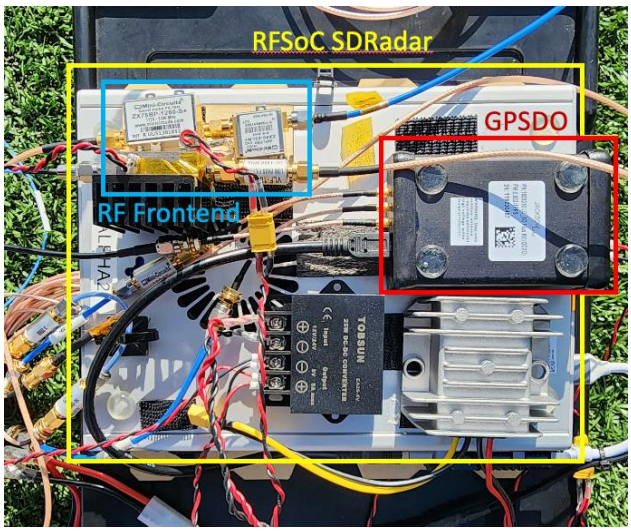

Figure 1. RFSoC-based SDRadar System. [6]

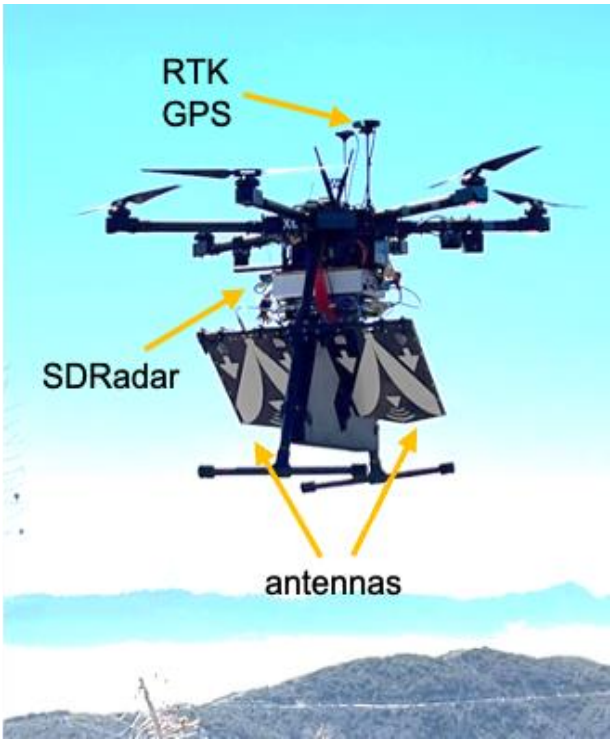

Figure 2. UAV-SDRadar testbed.

3 Monostatic Long-Range SAR Experiment

The system was tested in mountainous terrain near Charlton Flats Picnic Area in the Angeles National Forest on October 16th, 2022. The SDRadar operated at 3.2 GHz center frequency (S-Band) with about 200 MHz linear frequency modulated (LFM) chirp bandwidth, and 100 Hz pulse repetition frequency (PRF). The drone flew its path multiple times back and forth at 2 m/s speed and 100 m altitude during the experiment. The monostatic SAR image shown in Figure 3 was focused using a back-projection algorithm [8]. The SAR image size is 270 m along azimuth and 1 000 m along range, with an azimuth resolution of 0.3 m (degraded at ranges > 500 m) and a range resolution of 0.5 m. The 1-m resolution USGS DEM was used to improve the image focusing as well as to assess the image formation results. Backscatter modulation caused by topography and the Angeles Crest highway (CA-2) are well visible in the drone-SAR image.

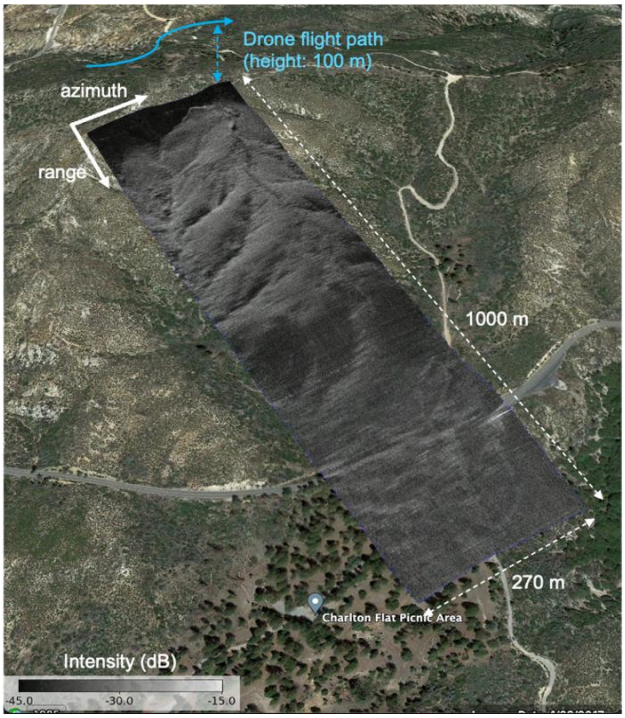

Figure 3. Long-range monostatic SAR image overlapped on Google Earth.

4 Bistatic SAR Experiment

4.1 One-stationary geometry

On March 3rd, 2023, DARTS team conducted a bistatic drone-SAR experiment at the Caltech South Athletic Field. Two SDRadars were used in the experiment, one mounted on the hexacopter drone and the other fixed on a tripod on the ground as shown in Figure 4. The SDRadars exchanged signals during the flight to ensure timing and synchronization of the radar signals required to process coherently the bistatic SAR image. The SDRadars operated at 1.25 GHz center frequency (L-band) with 85 MHz linear FM chirp bandwidth and 100 Hz PRF. Both radars transmitted and received alternatively, generating two bistatic data sets. The drone flew at 2 m/s and 25 ± 5 m altitude repeating the path multiple times facing North. Three corner reflectors were placed in the field.

The bistatic SAR was focused using the back-projection algorithm. The figure shows the bistatic SAR image obtained by the ground-SAR on transmission and the drone-SAR on reception. The main factors that affect focusing performance are the accuracy of the navigation data and the SNR of the synchronization link. The accuracy of the navigation data was enhanced by Post-Processed Kinematic GPS

(PPK GPS) position estimation. The synchronization link described in [9] was employed for these experiments. The bistatic drone-SAR image in Figure 5 shows well-focused corner reflectors and other visible surrounding structures such as buildings and fences. The image size is 300 m in range, and 200 m in azimuth. The impulse responses to a corner reflector in in range and azimuth is shown in Figure 6.

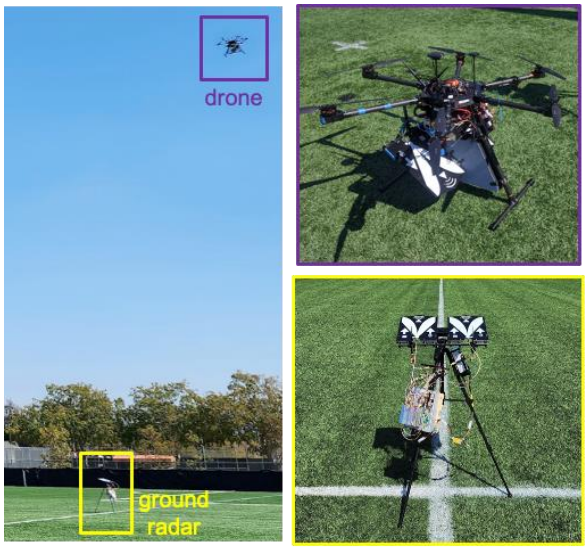

Figure 4. Bistatic SAR geometry with a UAV-SDRadar unit and a ground SDRadar unit.

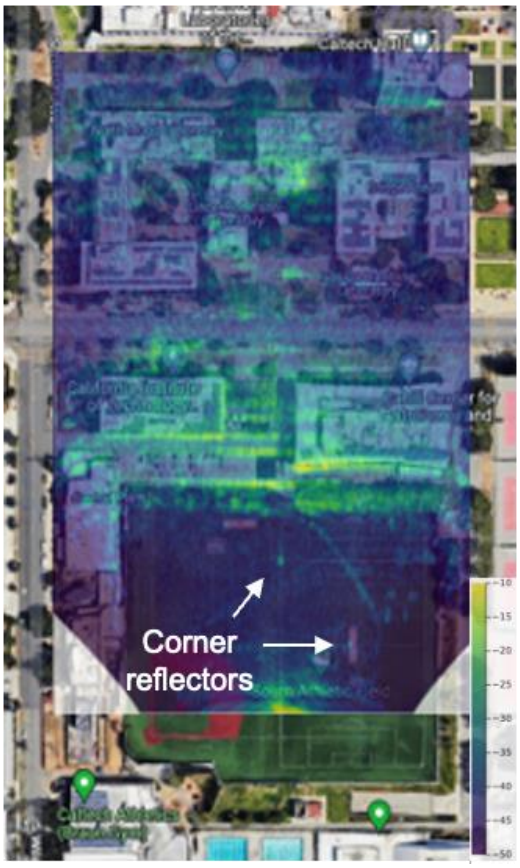

Figure 5. Bistatic SAR image overlaid on Google Maps.

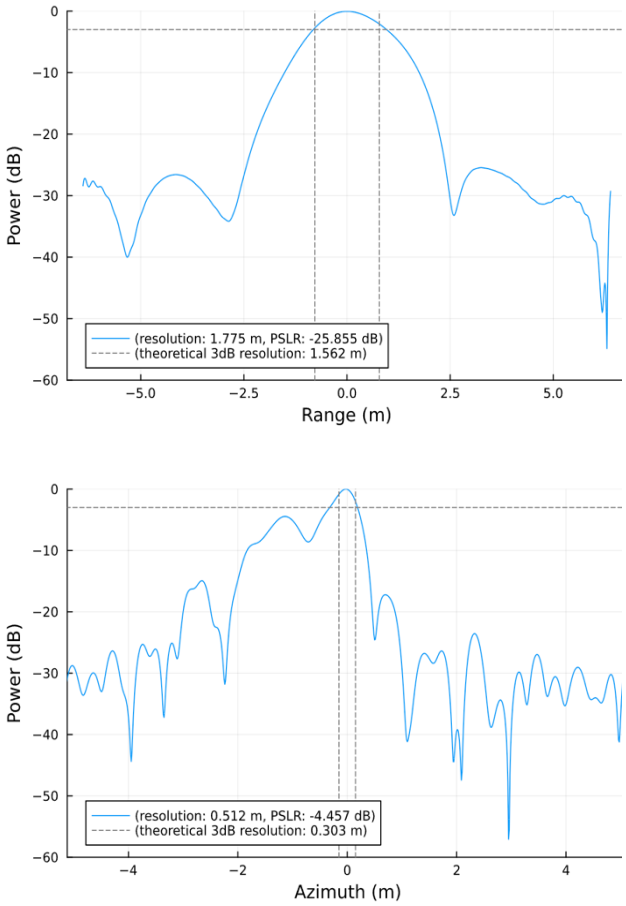

Figure 6. The impulse response in range (top) and in azimuth (bottom).

4.2 Tandem-flight geometry

On October 25th, 2023, DARTS team conducted a two-drone bistatic SAR experiment that the two drones flew simultaneously during the acquisition at the Caltech South Athletic Field. Two identical SDRadar and the UAV platform test beds were flown, as shown in Figure 7, to enable the simultaneous flight of two drones for acquiring bistatic data. The UAVs flew at 2 m/s speed and 30 m altitude, maintaining the displacement between them in all three axes; along-track, cross-track, and altitude. The SDRadars operated at a center frequency of 1.25 GHz (L-band), a 300 MHz LFM bandwidth, and a PRF of 100 Hz. Both radars alternately transmitted and received, delivering two bistatic datasets. The focused bistatic SAR intensity image is shown in Figure 8. The image size is 600 m in range, and 200 m in azimuth. The objects such as corner reflectors, temporarily installed fences, a soccer goal, and a bench appear prominently in the SAR image, confirming the system's ability to capture fine details of the observed scene.

Figure 7. Two-UAV bistatic UAV-SDRadar testbed (left) and the simultaneous flight during the acquisition (right).

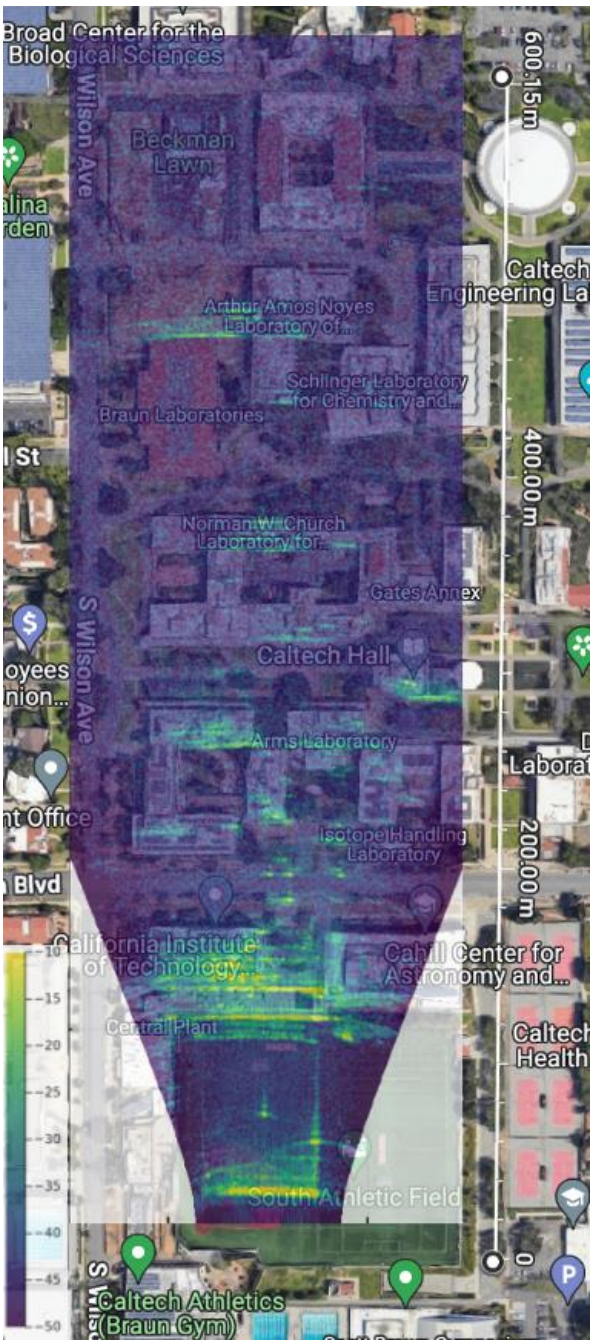

Figure 8. Two-UAV bistatic SAR image overlaid on Google Maps.

5 Discussions

5.1 Position data accuracy

An additional monostatic SAR experiment took place at Caltech South Athletic Field on December 9th, 2022. This experiment was aimed to acquire SAR data with enhanced drone position accuracy using PPK postprocessing. The SDRadar operated at a center frequency of 1.25 GHz (L-band) with a linear FM chirp bandwidth of 85 MHz and a PRF of 100 Hz. The UAV flew a repeated path facing South at 2 m/s and 50 ± 5 m altitude, and two corner reflectors were placed in the field.

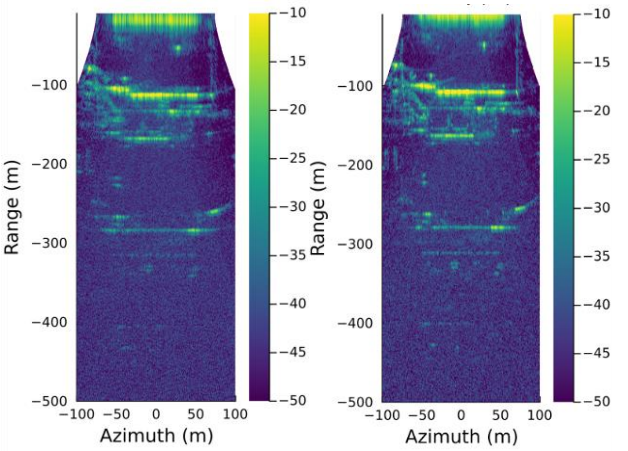

Figure 9. Monostatic SAR image before (left) and after (right) applying RTK post processing.

Figure 10. The impulse responses in range (top), and in azimuth (bottom)

The resulting monostatic SAR image shown in Figure 9 (right) is sharply focused compared to Figure 9 (left), with the improved accuracy of the UAV position data obtained through PPK postprocessing. The impulse response to a corner reflector before and after the PPK postprocessing is compared in Figure 10. The PPK postprocessing particularly enhanced the azimuth resolution.

5.2 Interferometric results

The enhanced position accuracy achieved through PPK postprocessing enabled the formation of a monostatic repeat-pass interferogram. In this experiment, a diverse set of flight paths with different altitudes was executed, including 45, 50, and 55 m. Despite the UAV maintaining a consistent preset altitude in some paths, the presence of motion disturbance and navigation errors introduced altitude offsets, consequently forming interferometric baselines sufficient to create spatial fringes. The resulting interferogram is illustrated in Figure 11 (left).

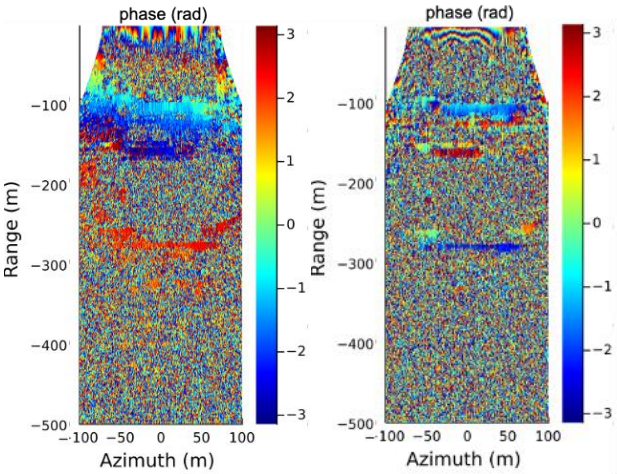

Figure 11. Repeat-pass monostatic interferogram with baseline of 0.3 m (left) and 4.8 m (right).

The repeat-pass bistatic interferogram shown in Figure 12 (left) was generated using the data collected from the two-drone bistatic experiment, as detailed in section 4.2. Similarly to the repeat-pass monostatic interferogram, the repeated UAV flight paths, set at the same altitude, induced a baseline due to motion disturbance and navigation offset errors, resulting in a baseline of 0.3 m.

The bistatic data set, radar A transmits and radar B receives, radar B transmits and radar A receives, was acquired simultaneously in this experiment, which generates single-pass interferogram shown in Figure 12 (right).

Despite the application of PPK postprocessing, the additional motion error sources with the utilization of two UAVs compared to the one-UAV experiments degrades the quality of the interferogram. This underscores the necessity for heightened precision in position data and synchronization, particularly in the context of bi- or multi-static interferometry, emphasizing the critical role of these factors in achieving reliable and accurate interferogram results.

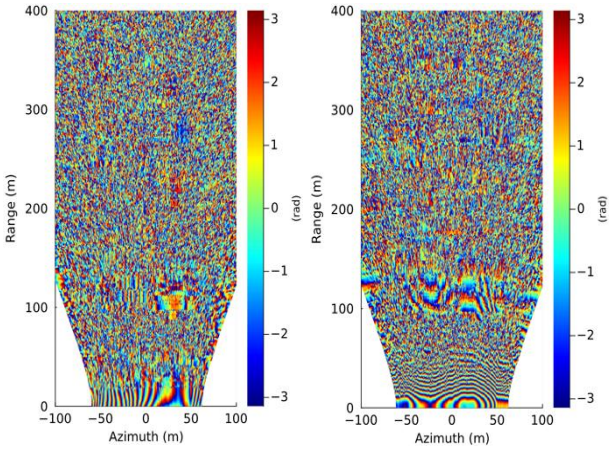

Figure 12. Bistatic interferogram; repeat-pass (left), and single-pass (right)

5.3 Synchronization

Synchronizing the multiple radars with independent local oscillators is challenging for both bi- and multi-static SAR configurations. For the current experiments, the synchronization link described in [9] is being utilized. However, additional work to reduce the timing synchronization error by incorporating phase information alongside time-of-flight information needs to be done. Also, it is recommended to explore diverse approaches to synchronization within the research community, taking into account both performance and efficiency considerations.

6 Conclusion

The DARTS project led by NASA Jet Propulsion Laboratory aims to demonstrate the potential of bi- or multi-static SAR for high-resolution 3D imaging of STV and SDC. By utilizing UAVs as SAR platforms and RFSoC based SDRadar, the project has achieved significant progress in hardware development, data acquisition, and processing techniques. The experiments successfully demonstrated monostatic and bistatic SAR and InSAR with the improved position accuracy using PPK postprocessing and synchronization technique. Future efforts will focus on acquiring single-pass bistatic interferograms and tomograms for SDC and STV measurements through either drone-based or airborne platforms.

7 Acknowledgements

The research reported here was carried out in part at the Jet Propulsion Laboratory, Caltech, under a contract with the National Aeronautics and Space Administration (80NM0018D0004). We would like to thank ESTO for providing the funds.

8 Literature

[1] I. Woodhouse, *Introduction to Microwave Remote Sensing*, Chapman and Hall/CRC, Boca Raton, 2017.

[2] A. Reigber and A. Moreira, "First demonstration of airborne SAR tomography using multibaseline L-band data," *IEEE Transaction on Geoscience and Remote Sensing*, vol. 30, no. 5, pp. 2142-2152, Sep. 2000.

[3] A. Moreira, P. Prats-Iraola, M. Younis, G. Krieger, I. Hajnsek, and K. P. Papathanassiou, "A tutorial on synthetic aperture radar," *IEEE Geoscience and Remote Sensing Magazine*, vol. 1, no. 1, pp. 6-43, Mar 2013.

[4] S. Tebaldini, M. M. d'Alessandro, L. M.H. Ulander, P. Bennet, A. Gustavsson, A. Coccia, K. Macedo, M. Disney, P. Wilkes, H.-J. Spors, N. Schumacher, J. Hanuš, J. Novotný, B. Brede, H. Bartholomeus, A. Lau, J. van der Zee, M. Herold, D. Schuettemeyer, K. Scipal, "TomoSense: A unique 3D dataset over temperate forest combining multi-frequency mono- and bi-static tomographic SAR with terrestrial, UAV and airborne lidar, and in-situ forest census," *Remote Sensing of Environment*, vol. 290, pp. 113532, 2023.

[5] M. Lavalle, I. Seker, J. Ragan, E. Loria, R. Ahmed, B. P. Hawkins, S. Prager, D. Clark, R. Beauchamp, M. Haynes, P. Focardi, N. Chahat, M. Anderson, K. Matsuka, V. Capuano, and S.-J. Chung, "Distributed aperture radar tomographic sensors (DARTS) to map surface topography and vegetation structure," in *2021 IEEE International Geoscience and Remote Sensing Symposium*, July 2021.

[6] B. Hawkins, M. Anderson, S. Prager, S.-J. Chung, and M. Lavalle, "Experiments with small UAS to support SAR tomographic mission formulation," in *2021 IEEE International Geoscience and Remote Sensing Symposium*, July 2021.

[7] S. Prager, B. Hawkins, M. Anderson, S.-J. Chung, and M. Lavalle, "Development of ultra-wideband software defined radar testbed to support SAR tomographic mission formulation," in *2021 IEEE International Geoscience and Remote Sensing Symposium*, July 2021.

[8] O. Frey, C. Magnard, M. Ruegg, and E. Meier, "Focusing of airborne synthetic aperture radar data form highly nonlinear flight tracks," *IEEE Transactions on Geoscience and Remote Sensing*, vol. 47, no. 6, pp. 1844-1858, 2009.

[9] S. Prager, M. S. Haynes, and M. Moghaddam, "Wireless subnanosecond RF synchronization for distributed ultrawideband software-defined radar networks," *IEEE Transactions on Microwave Theory and Techniques*, vol. 68, no. 11, pp. 4787-4804, 2020.